

Depinning frequency in a heavily neutron-irradiated MgB₂ sample

M. Bonura^a, A. Agliolo Gallitto^a, M. Li Vigni^{a,*},
A. Martinelli^b,

^a*CNISM and Dipartimento di Scienze Fisiche e Astronomiche, Università di Palermo, via Archirafi 36, 90123 Palermo, Italy*

^b*CNR-INFM-LAMIA and Dipartimento di Fisica, Università di Genova, Via Dodecaneso 33, I-16146 Genova, Italy*

Abstract

The magnetic-field-induced variations of the microwave surface resistance have been investigated in a heavily neutron-irradiated MgB₂ sample, in which the irradiation has caused the merging of the two gaps into a single value. The experimental results have been analyzed in the framework of the Coffey and Clem model. By fitting the experimental data, we have determined the field dependence of the depinning frequency, ω_0 , at different values of the temperature. Although the pinning is not particularly effective, the value of ω_0 obtained at low temperatures is considerably higher than that observed in conventional low-temperature superconductors.

Key words: Depinning frequency, MgB₂, Microwave surface resistance

PACS: 74.25.Ha, 74.25.Nf, 74.60.Ge

1 Introduction

Investigation of fluxon dynamics in type-II superconductors is of great interest for both fundamental and applicative aspects. From the basic point of view, it gives information on the relative magnitude of elastic and viscous forces, which rule the motion regime of the fluxon lattice [1,2,3,4,5,6]. From the technological point of view, it allows determining the magnetic-field-induced energy losses, which have important implication in a large variety of superconductor-based devices [7].

* Tel.: +39 0916234208; fax: +39 0916162461; e-mail: livigni@fisica.unipa.it

A suitable method to investigate the fluxon dynamics consists in determining the magnetic-field-induced variations of the microwave (mw) surface resistance, R_s [2]. In the absence of static magnetic fields, the variation with the temperature of the condensed-fluid density determines the temperature dependence of R_s . On the other hand, the field dependence of R_s in superconductors in the mixed state is determined by the presence of fluxons, which bring along normal fluid in their cores, as well as the fluxon motion [1,2,3,4,5,6,8,9,10]. Measurements of the high-frequency em response allow to conveniently investigate the vortex dynamics because they probe the vortex response at very low currents, when vortices undergo reversible oscillations and are less sensitive to flux-creep processes.

In a fluxon lattice driven by mw currents, the regime of vortex motion is ruled by the relative magnitude of the viscous-drag force, due to the presence of the normal cores, and the restoring-pinning force, which hinders the motion of fluxons. A very important parameter of the vortex dynamics is the depinning frequency, ω_0 , which separates two regimes of vortex motion. When the frequency of the driving field, ω , is much larger than ω_0 , the viscous-drag force dominates the restoring-pinning force; in this case, the vortex resistivity [2] is real and the motion of fluxons is highly dissipative. On the contrary, for $\omega \ll \omega_0$ the vortex resistivity is imaginary and the energy losses are strongly reduced. Measurements of the depinning frequency have been performed in both conventional [1,3,11] and high- T_c superconductors [3,4,6,12]. For temperatures lower enough than T_c and applied magnetic fields smaller enough than H_{c2} , conventional superconductors exhibit depinning frequency of the order of MHz, while much higher values ($\gtrsim 10$ GHz) have been reported for cuprate high- T_c superconductors.

Since the first studies on MgB_2 , different authors have highlighted several anomalies in the field-induced variations of the mw surface impedance, especially at low temperatures and magnetic fields much lower than the upper critical field [13,14,15,16,17,18]. These studies have established that the standard theories are inadequate to describe the fluxon dynamics in the two-gap MgB_2 , in wide ranges of temperatures and magnetic fields. This is most likely due to the peculiar properties of the mixed state of MgB_2 , related to the presence of the two distinct gaps [19,20,21,22,23].

Recently, polycrystalline Mg^{11}B_2 samples irradiated up to very high neutron fluence have extensively been investigated [24,25,26,27,28]. It has been shown that irradiation up to exposure levels of $2 \times 10^{18} \text{ cm}^{-2}$ leads to an improvement in the upper critical field and in the field dependence of the critical current density. On further increasing the neutron fluence, all the superconducting properties, such as T_c , H_{c2} , J_c , are reduced. Furthermore, measurements of specific heat, as well as point-contact spectroscopy, have shown that in the sample irradiated at the highest fluence ($1.4 \times 10^{20} \text{ cm}^{-2}$) the two gaps merge

into a single value [27,28]. Very recently [26], transmission-electron-microscopy studies have shown that neutron irradiation creates nanometric amorphous regions within the MgB₂ crystallites, whose density increases on increasing the neutron fluence. In samples irradiated with neutron fluence $\leq 10^{19}$ cm⁻², such defects act as additional pinning centers. The field dependence of the critical current density observed in these samples has been quantitatively justified by considering the contribution of two pinning mechanisms, one arising from grain boundaries, which is also present in the pristine sample, and the other arising from the defects induced by irradiation. On the contrary, the results of $J_c(B)$ obtained in the samples irradiated with neutron fluence larger than 10^{19} cm⁻² have not fully been justified; in this case, the measured J_c values are even lower than those expected from the grain-boundary contribution. A thorough understanding of the pinning mechanisms that come into play in the heavily irradiated samples is not yet achieved.

In this paper, we report a detailed investigation of the magnetic-field-induced variations of the microwave surface resistance of a MgB₂ sample irradiated at the neutron fluence of 1.4×10^{20} cm⁻². Preliminary results obtained in this sample have shown that the mw losses can be justified in the framework of standard models for vortex dynamics [18]. Here, we report the results obtained in a wide range of temperatures (4.2 K $\div T_c$), from which we determine the temperature and the magnetic-field dependencies of the depinning frequency. The investigation allowed us to determine also the field dependence of the pinning coefficient and the radius of action of the pinning potential.

2 Experimental apparatus and sample

The field-induced variations of the mw surface resistance has been investigated in a bulk sample of Mg¹¹B₂ irradiated at very high neutron fluence (1.4×10^{20} cm⁻²). The procedure for the preparation and irradiation of the sample is reported in detail elsewhere [25,27]. The sample has been prepared by direct synthesis from Mg (99.999% purity) and crystalline isotopically enriched ¹¹B (99.95% purity), with a residual ¹⁰B concentration lower than 0.5%. The use of isotopically enriched ¹¹B makes the penetration depth of the thermal neutrons greater than the sample thickness; this guarantees that the irradiation effects are almost homogeneous over the sample. Several superconducting properties of the sample have been reported in Refs. [24,25,26,27,28]. For simplicity and easy of comparison, we label the sample as P6, according to Refs. [18,24,25,26,27,28]. Point-contact-spectroscopy [28] and specific-heat [27] measurements have shown that the neutron-irradiation process determined in this sample a merging of the two gaps into a single value.

The sample has a nearly parallelepiped shape with $w \approx 1.1$ mm, $t \approx 0.8$ mm

and $h \approx 1.4$ mm; the effect of the neutron irradiation on this sample led to a worsening of several properties. The superconducting transition is characterized by $T_c^{onset} \approx 9.1$ K and $\Delta T_c \approx 0.3$ K (from 10% to 90% of the normal-state resistivity); the residual resistivity ratio is $RRR = 1.1$; the critical current density at zero magnetic field is $J_{c0} \approx 3 \times 10^4$ A/cm², it exhibits a monotonic decrease with the magnetic field, following roughly an exponential law. The upper critical field is isotropic and its value at $T = 5$ K is $\mu_0 H_{c2} \approx 2$ T. The measured value of the normal-state resistivity is $\rho_n(40 \text{ K}) = 130 \mu\Omega \text{ cm}$; however, as suggested by Rowell [29], the real value of the residual normal-state resistivity can be different because of reduction of the effective current-carrying cross-sectional area of the sample due to the grain boundaries. The rescaled value of the residual normal-state resistivity, corrected by the Rowell's criterion, is $\rho_n(T_c) \approx 90 \mu\Omega \text{ cm}$ [25].

Although the superconducting transition of the sample is sharp, it results $\Delta T_c/T_c \approx 0.03$. Since the distribution of T_c may affect the temperature dependence of the mw surface resistance near T_c , we have determined the T_c distribution function by measurements of the AC susceptibility at 100 kHz. We have found that the first derivative of the real part of the AC susceptibility can be described by a Gaussian distribution function of T_c , centered at $T_{c0} = 8.5 \pm 0.1$ K with $\sigma_{T_c} = 0.2 \pm 0.05$ K. In the following, we will use this distribution function to quantitatively discuss the results.

The mw surface resistance has been measured using the cavity-perturbation technique [2]. A copper cavity, of cylindrical shape with golden-plated walls, is tuned in the TE_{011} mode resonating at $\omega/2\pi \approx 9.6$ GHz. The sample is located in the center of the cavity by a sapphire rod, in the region in which the mw magnetic field is maximum. The cavity is placed between the poles of an electromagnet which generates DC magnetic fields up to $\mu_0 H_0 \approx 1$ T. The sample and the field geometries are shown in Fig. 1a; the DC magnetic field, \mathbf{H}_0 , is perpendicular to the mw magnetic field, \mathbf{H}_ω . When the sample is in the mixed state, the induced mw current causes a tilt motion of the vortex lattice [9]; Fig. 1b schematically shows the motion of a flux line.

The surface resistance of the sample is given by

$$R_s = \Gamma \left(\frac{1}{Q_L} - \frac{1}{Q_U} \right),$$

where Q_L is the quality factor of the cavity loaded with the sample, Q_U that of the empty cavity and Γ the geometry factor of the sample.

The quality factor of the cavity has been measured by an hp-8719D Network Analyzer. The surface resistance has been measured as a function of the DC magnetic field, at fixed temperatures. All the measurements have been performed at very low input power; the estimated amplitude of the mw magnetic field in the region in which the sample is located is of the order of $0.1 \mu\text{T}$.

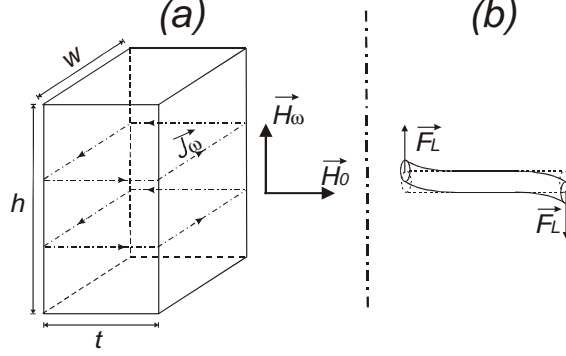


Fig. 1. (a) Field and current geometry at the sample surface. (b) Schematic representation of the motion of a flux line.

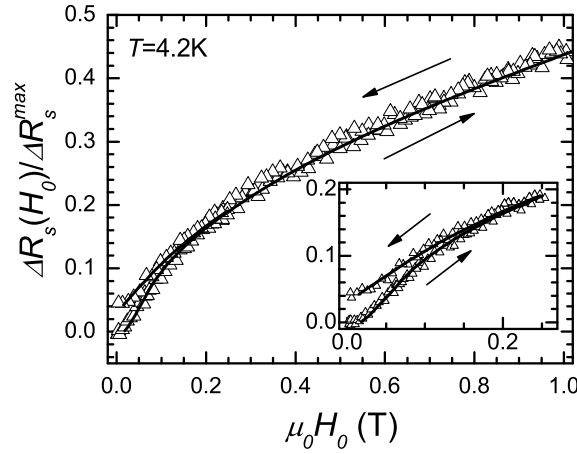


Fig. 2. Field-induced variations of R_s at $T = 4.2$ K. $\Delta R_s(H_0) \equiv R_s(H_0, T) - R_{res}$, where R_{res} is the residual mw surface resistance at $T = 2.5$ K and $H_0 = 0$; $\Delta R_s^{max} \equiv R_n - R_{res}$, where R_n is the normal-state value of R_s at $T = T_c$. The lines are the best-fit curves obtained, as explained in Ref. [18], with $\mu_0 H_{c2} = 1.71$ T, $\omega_0/\omega = 0.67$ and the field dependence of the critical current density reported in Ref. [25]. The inset shows a minor hysteresis loop obtained by sweeping H_0 from 0 to 0.25 T and back, along with the best-fit curve.

3 Experimental results

The field-induced variations of R_s have been investigated at different temperatures. For each measurement, the sample was ZFC down to the desired value of temperature; the DC magnetic field was increased up to a certain value and, successively, decreased down to zero. Figs. 2, 3 and 4 show the field-induced variations of R_s , at different temperatures. In all the figures, $\Delta R_s(H_0) \equiv R_s(H_0, T) - R_{res}$, where R_{res} is the residual mw surface resistance at $T = 2.5$ K and $H_0 = 0$; moreover, the data are normalized to the maximum variation, $\Delta R_s^{max} \equiv R_n - R_{res}$, where R_n is the normal-state value of the surface resistance at $T = T_c$. In the figures, the continuous lines are the best-fit curves obtained by the model described in Sec. 4.

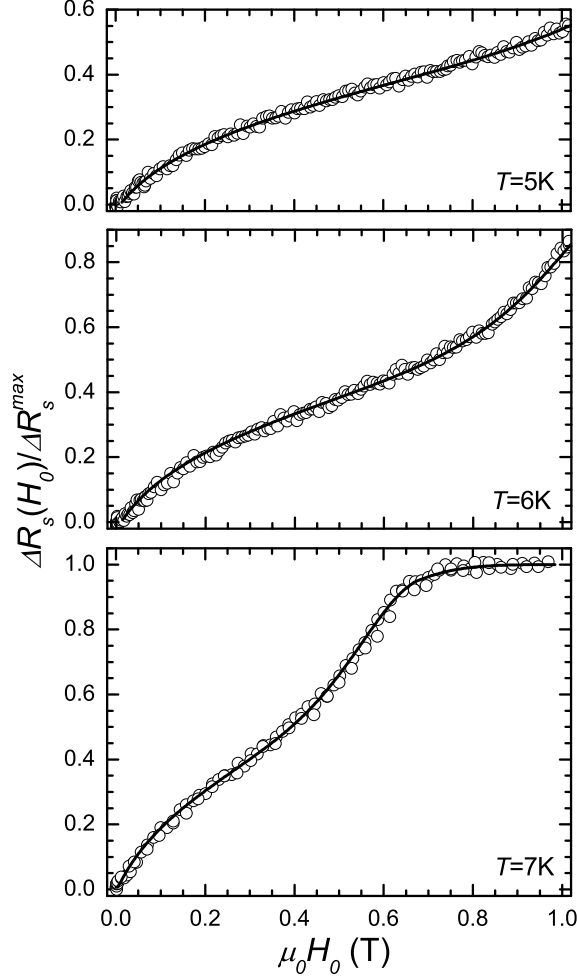


Fig. 3. Field-induced variations of R_s for the MgB₂ sample, at different values of the temperature. $\Delta R_s(H_0) \equiv R_s(H_0, T) - R_{res}$; $\Delta R_s^{max} \equiv R_n - R_{res}$. The lines are the best-fit curves obtained as explained in Sec. 4.

From Fig. 2 one can see that at $T = 4.2$ K the $R_s(H_0)$ curve exhibits a magnetic hysteresis for H_0 lower than ≈ 0.18 T. The hysteresis is ascribable to the different magnetic induction at increasing and decreasing DC fields, due to the critical state of the vortex lattice [30,31,32]. These results have been reported and discussed in Ref. [18]. In order to fit the data, we have determined the B profile inside the sample due to the critical state and calculated a proper averaged value of $R_s(B)$ over the whole sample. The lines in the figure are the best-fit curves.

For $T \geq 5$ K the $R_s(H_0)$ curves are reversible, indicating that at these temperatures the critical-state effects of the fluxon lattice are negligible. However, we would like to remark that, for samples of millimetric size, the sensitivity of our experimental apparatus allows detecting hysteresis in the $R_s(H_0)$ curves for $J_c \gtrsim 10^4$ A/cm².

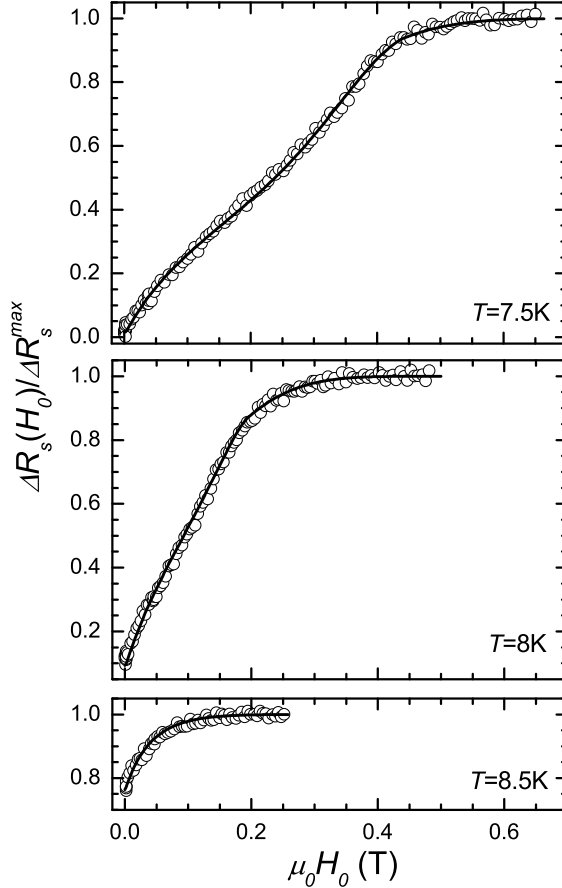


Fig. 4. Field-induced variations of R_s for the MgB₂ sample, at different values of the temperature. $\Delta R_s(H_0) \equiv R_s(H_0, T) - R_{res}$; $\Delta R_s^{max} \equiv R_n - R_{res}$. The lines are the best-fit curves obtained as explained in Sec. 4.

4 Discussion

Microwave losses induced by static magnetic fields have been investigated by several authors [1,2,3,4,5,6,7,8,9,32,33]. At low temperatures and for applied magnetic fields lower enough than the upper critical field, the main contribution arises from the fluxon motion; however, it has been pointed out that a noticeable contribution can arise from the presence of normal fluid, especially at temperatures near T_c and for magnetic fields of the same order of $H_{c2}(T)$.

In the London local limit, the surface resistance is proportional to the imaginary part of the complex penetration depth, $\tilde{\lambda}$, of the em field:

$$R_s = -\mu_0 \omega \text{Im}[\tilde{\lambda}(\omega, B, T)]. \quad (1)$$

The complex penetration depth has been calculated in different approximations [8,9]. Coffey and Clem (CC) have elaborated a comprehensive theory for the electromagnetic response of superconductors in the mixed state, in the

framework of the two-fluid model of superconductivity [8]. The CC theory has been developed under the assumption that the induction field, B , is uniform in the sample; so, it is valid for $H_0 > 2H_{c1}$ whenever the fluxon distribution can be considered uniform within the AC penetration depth.

In the linear approximation, $H_\omega \ll H_0$, $\tilde{\lambda}(\omega, B, T)$ expected from the CC model is given by

$$\tilde{\lambda}(\omega, B, T) = \sqrt{\frac{\lambda^2(B, T) + (i/2)\tilde{\delta}_v^2(\omega, B, T)}{1 - 2i\lambda^2(B, T)/\delta_{nf}^2(\omega, B, T)}}, \quad (2)$$

with

$$\lambda(B, T) = \frac{\lambda_0}{\sqrt{[1 - w_0(T)][1 - B/B_{c2}(T)]}}, \quad (3)$$

$$\delta_{nf}(\omega, B, T) = \frac{\delta_0(\omega)}{\sqrt{1 - [1 - w_0(T)][1 - B/B_{c2}(T)]}}, \quad (4)$$

where λ_0 is the London penetration depth at $T = 0$, δ_0 is the normal-fluid skin depth at $T = T_c$, $w_0(T)$ is the fraction of normal electrons at $H_0 = 0$; in the Gorter and Casimir two-fluid model $w_0(T) = (T/T_c)^4$.

$\tilde{\delta}_v$ is the effective complex skin depth arising from the vortex motion; it depends on the relative magnitude of the viscous and restoring-pinning forces. $\tilde{\delta}_v$ can be written in terms of two characteristic lengths, δ_f and λ_c , arising from the contributions of the viscous and the restoring-pinning forces, respectively:

$$\frac{1}{\tilde{\delta}_v^2} = \frac{i}{2\lambda_c^2} + \frac{1}{\delta_f^2}, \quad (5)$$

where

$$\lambda_c^2 = \frac{B\phi_0}{\mu_0 k_p}, \quad (6)$$

$$\delta_f^2 = \frac{2B\phi_0}{\mu_0 \omega \eta}, \quad (7)$$

with k_p the restoring-force coefficient, η the viscous-drag coefficient and ϕ_0 the quantum of flux.

The effectiveness of the two terms in Eq. (5) depends on the ratio $\omega_0 = k_p/\eta$, which defines the depinning frequency [1]. In terms of ω_0 , Eq. (5) becomes

$$\frac{1}{\tilde{\delta}_v^2} = \frac{1}{\delta_f^2} \left(1 + i \frac{\omega_0}{\omega} \right). \quad (8)$$

When $\omega \ll \omega_0$, the fluxon motion is ruled by the restoring-pinning force. On the contrary, for $\omega \gg \omega_0$, the fluxon motion takes place around the minimum of the pinning-potential well and, consequently, the restoring-pinning force is nearly ineffective; so, the contribution of the viscous-drag force predominates

and the induced em current makes fluxons move in the flux-flow regime. In the latter case, enhanced field-induced energy losses are expected.

The theory above discussed is strictly valid when B is uniform inside the sample. When fluxons are in the critical state, the assumption of uniform B is no longer valid and the CC theory does not correctly describe the field-induced variations of R_s . Recently, we have investigated the field-induced variations of the mw surface resistance in superconductors in the critical state and have accounted for the magnetic hysteresis in the $R_s(H_0)$ curves [32,33]. The details of the procedure we have followed to account for the experimental results of Fig. 2, where the critical-state effects are important, are reported in Refs. [18]. Since $R_s(H_0)$ in the investigated sample does not show hysteresis in a wide range of temperatures, we do not discuss here on this procedure.

The expected value of the normalized surface resistance depends on several parameters, such as the ratio λ_0/δ_0 , the temperature dependence of the normal-fluid density $w_0(T)$, $H_{c2}(T)$, the depinning frequency and its field dependence. However, λ_0/δ_0 and the temperature dependence of the normal-fluid density determine the value of $R_s(T)$ at $H_0 = 0$. In Ref. [18] we have shown that the $R_s(T)$ curve at $H_0 = 0$ can be quite well justified assuming valid the Gorter and Casimir two-fluid model, with λ_0/δ_0 values ranging from 0.04 to 0.15, provided that distribution of T_c in the sample is taken into account. The large uncertainty of λ_0/δ_0 is due to the fact that the T_c distribution broadens the $R_s(T)$ curve, hiding the λ_0/δ_0 effects.

At fixed temperature, the expected field-induced variations of R_s depend on $\omega_0(B)$ and $H_{c2}(T)$. The temperature dependence of H_{c2} has been reported in Refs. [18,25]; it can be described by the law

$$H_{c2}(T) = H_{c20}[1 - (T/T_c)^\alpha], \quad (9)$$

with $\mu_0 H_{c20} = (2.2 \pm 0.2)$ T, $\alpha = 1.9 \pm 0.3$ and $T_c = (8.9 \pm 0.2)$ K.

By using this relation for $H_{c2}(T)$, it is possible to determine the field dependence of the depinning frequency by fitting the experimental isothermal $R_s(H_0)$ curves.

For $T \geq 5$ K, the $R_s(H_0)$ curves do not show hysteresis, suggesting that the effects of the critical state are negligible. Since on increasing the temperature the effects of the distribution of T_c become more and more important, to fit the experimental data we have averaged the expected $R_s(H_0)$ curves [calculated by Eqs. (1-4)] over the T_c distribution; have used Eq. (9) for $H_{c2}(T)$; have taken ω_0 as parameter dependent on H_0 . Moreover, we have used the following approximate expression for the magnetization:

$$M = -H_p + \frac{H_p}{H_{c2} - H_p}(H_0 - H_p) \quad (10)$$

and consequently

$$B = \mu_0 \left(1 + \frac{H_p}{H_{c2} - H_p} \right) (H_0 - H_p), \quad (11)$$

where H_p is the first-penetration field.

H_p can be directly deduced from the experimental curves, measuring the applied magnetic field at which R_s starts to increase; its temperature dependence has been reported in Ref. [18]. The best-fit curves of $R_s(H_0)$ are reported in Figs. 2, 3 and 4; the field dependence of ω_0/ω , by which the best fit has been obtained, is reported in Fig. 5, at different temperatures. We remark that we have investigated the field-induced variations of R_s down to $T = 2.5$ K; the results of the depinning frequency for $T < 4.2$ K are not reported here because, within the experimental uncertainty, they are the same of those obtained at $T = 4.2$ K.

Considering the frequency of the mw field ($\omega/2\pi \simeq 9.6$ GHz), from ω_0/ω we obtain that the depinning frequency at low fields is $\omega_0/2\pi \approx 6$ GHz. For $T \leq 5$ K, ω_0 is independent of B in a wide field range; on increasing the temperature, this field range shrinks. Moreover, for applied fields larger than a threshold value, dependent on T , the fluxon lattice moves in the flux-flow regime ($\omega_0 \ll \omega$); on increasing the temperature, this threshold field decreases; eventually, at $T > 8$ K the fluxon lattice moves in the flux-flow regime in the whole field range investigated.

Two regimes of vortex pinning can be identified: individual pinning and collective pinning. Individual pinning is realized at low fields, when there are few vortices and many pinning sites per vortex. In this regime, ω_0 is expected to be independent of B . Collective pinning is realized at higher fields when the vortex concentration is high and there are many vortices per pinning site; in this regime, ω_0 gets lower values and depends on B [2]. Our experimental

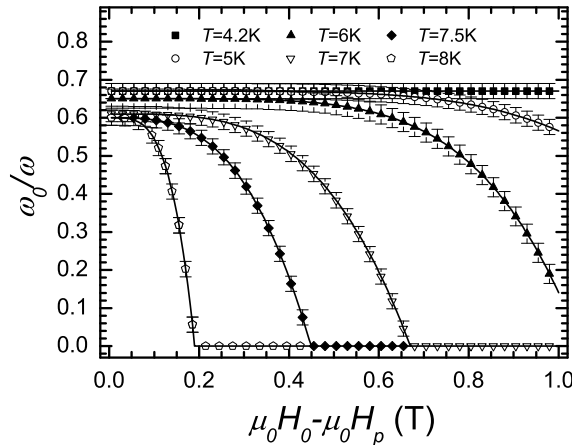


Fig. 5. Magnetic field dependence of the depinning frequency, obtained by fitting the experimental $R_s(H_0)$ curves, at different temperatures.

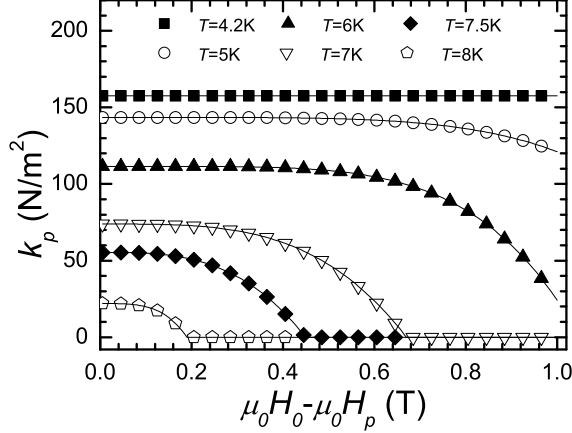


Fig. 6. Deduced field dependence of the pinning coefficient k_p , at different temperatures.

results indicate that for $T \lesssim T_c/2$ individual pinning is realized in almost the whole field range investigated.

Since the field-induced mw losses depend on the relative magnitude of the viscous and restoring-pinning forces, our analysis does not allow to obtain independently the coefficients k_p and η , but only the ratio $\omega_0 = k_p/\eta$. However, the investigated sample has shown properties that can be quite well accounted for by conventional models; so, one can deduce k_p by supposing valid the Bardeen-Stephen relation [34]

$$\eta(T) = \frac{\phi_0 \mu_0 H_{c2}(T)}{\rho_n}, \quad (12)$$

where ρ_n is the normal-state resistivity at $T = T_c$.

Both $\rho_n(T_c)$ and $H_{c2}(T)$ of the investigated sample have been already determined: $\rho_n(T_c) \approx 90 \mu\Omega \text{ cm}$ [25] and $H_{c2}(T)$ is given by Eq. (9). The deduced field dependence of k_p is shown in Fig. 6, at different values of the temperature.

An upper limit of the pinning constant, k_p^{max} , can be obtained by equating the energy density per unit length of the vortex core, $B_c^2 \xi^2 \pi / 2 \mu_0$, to the elastic stored energy density per unit length of the vortex core, $k_p^{max} \xi^2 / 2$ [35]. It follows:

$$k_p^{max} = \frac{\pi B_c^2}{\mu_0}, \quad (13)$$

where B_c is the thermodynamic critical field.

At low temperatures, from B_{c1} and B_{c2} we estimate that the thermodynamic critical field is of the order of 100 mT; so, from Eq. (13) we estimate k_p^{max} to be of the order of 10^4 N/m^2 . The values of k_p we have obtained from the experimental data are two orders of magnitude lower than k_p^{max} deduced from Eq. (13); so, we infer that pinning is not particularly effective in the

investigated sample. This finding is consistent with the low J_c value responsible for the weak hysteretic behavior of R_s reported in Fig. 2.

From simultaneous measurements of the pinning constant and critical current density it is possible to estimate the average radius of action, r_p , of the pinning potential, $U(r)$. The pinning constant, $k_p = d^2U/dr^2$, is related to the critical current density; since $J_c = \phi_0^{-1}dU/dr|_{r_p}$, one obtains $J_c = k_p r_p / \phi_0$ [2]. By using the value of $J_c(5\text{ K})$ reported in Ref. [25] and the value we obtained for k_p , it results $r_p \approx 4\text{ nm}$. At applied fields of $\approx 1\text{ T}$, the estimated distance between vortices is $\sqrt{\phi_0/B} \approx 45\text{ nm}$; so, the deduced value of $r_p(5\text{ K})$ is much smaller than the distance between vortices. This finding confirms that, in our sample, for $T \leq 5\text{ K}$ individual pinning is realized in almost the whole field range investigated, consistently with the field-independent depinning frequency obtained at these temperatures (see Fig. 5).

It is widely accepted that in pristine MgB_2 bulk samples the pinning mechanism is ruled by grain boundaries [24,25,26,36,37]. Recently, it has been shown that neutron irradiation introduces defects in the form of amorphous regions of mean diameter $\sim 4\text{ nm}$ [26], uniformly distributed within the crystallites; the defect density increases on increasing the neutron fluence. Studies on the field dependence of the critical current density [24,26] have suggested that at moderate neutron-fluence levels ($\leq 1 \times 10^{19}\text{ cm}^{-2}$) these defects give a further contribution to the pinning, leading to an improvement of the critical current density, with respect to the values expected from grain-boundary pinning. The same effect has not been observed in samples irradiated with higher fluences; in this case, the measured J_c values are even lower than those expected by properly rescaling the grain-boundary contribution. Most likely, this is due to the different coherence length of the different samples: in samples exposed to neutron fluence $\leq 1 \times 10^{19}\text{ cm}^{-2}$ the defect dimension matches with the coherence length; in samples exposed to higher fluences the coherence length is larger than the defect size and, consequently, the defects are not effective for the fluxon pinning. The results we have obtained in the heavily irradiated sample confirm this conclusion; indeed, we have obtained small values of the pinning coefficient. So, despite the high concentration of defects, they do not contribute positively to the pinning.

The depinning frequency in the investigated sample is considerably higher than the values reported in the literature for conventional superconductors; for example, the depinning frequency in bulk niobium, which has comparable values of H_{c2} , is less than 10^8 Hz [2]. Since the values we have obtained for the pinning constant k_p are considerably lower than the upper limit k_p^{max} , the high value of ω_0 cannot surely be ascribed to strong pinning effects; so, we infer that it is ascribable to a low value of the viscosity coefficient. On the other hand, in this sample the residual normal-state resistivity is $\rho(T_c) = 90\ \mu\Omega\text{ cm}$; this high value of $\rho(T_c)$ has been ascribed to a reduced value of the electron

mean free path due to the presence of the defects induced by the neutron irradiation [25]. We suggest that it is just the high value of the normal-state resistivity responsible for the small viscosity coefficient that, in turn, gives rise to the high value of the depinning frequency.

5 Conclusion

We have measured the magnetic-field-induced variations of the mw surface resistance in a heavily neutron-irradiated Mg^{11}B_2 sample, in which the two gaps merged into a single value. The field dependence of R_s , at different values of the temperature, have been discussed in the framework of the Coffey and Clem model, with the temperature dependence of the normal-fluid density expected from the Gorter and Casimir two-fluid model.

By fitting the experimental data, we have determined the magnetic-field dependence of the depinning frequency at different temperatures. We have found that, for $T \lesssim T_c/2$ the depinning frequency ω_0 does not depend on the magnetic field, indicating that individual pinning is realized in the whole field range investigated; on increasing the temperature, the range of H_0 in which individual pinning occurs shrinks and ω_0 is field dependent above a certain threshold value of the applied field, depending on T . By supposing valid the Bardeen-Stephen relation for the viscosity coefficient, we have deduced the field dependence of the pinning coefficient at different temperatures; moreover, considering the value of the critical current density, we have deduced the radius of action of the pinning potential. Although the neutron-irradiation process created a high density of defects, our results show that the pinning is not particularly effective, consistently with the relatively low value of the critical current density reported for this sample; this finding is most likely due to the fact that the coherence length is larger than the mean size of the defects. Nevertheless, the deduced value of the depinning frequency is considerably higher than that reported for conventional SC, as bulk Nb. We suggest that this high value of ω_0 is due to the high value of the normal-state resistivity in the investigated sample, which is due to the reduced value of the electron mean free path because of the presence of the defects.

Acknowledgements

The authors are very glad to thank C. Ferdeghini and M. Putti for their interest to this work and helpfull suggestions; G. Lapis and G. Napoli for technical assistance.

References

- [1] J. I. Gittleman, B. Rosenblum, Phys. Rev. Lett. **16** (1966) 734.
- [2] M. Golosovsky, M. Tsindlekht, D. Davidov, Supercond. Sci. Technol. **9** (1996) 1, and Refs. therein.
- [3] M. Golosovsky, M. Tsindlekht, H. Chayet, D. Davidov, Phys. Rev. B **50** (1994) 470.
- [4] J. Owliaei, S. Shridar, J. Talvacchio, Phys. Rev. Lett. **69** (1992) 3366.
- [5] A. Dulčić, M. Požek, Physica C **218** (1993) 449.
- [6] S. Fricano, M. Bonura, A. Agliolo Gallitto, M. Li Vigni, L. A. Klinkova, N. V. Barkovskii, Eur. Phys. J. B **41** (2004) 313.
- [7] H. Weinstock, M. Nisenoff, Microwave Superconductivity, NATO Science Series, Series E: Applied Science - Vol. 375, Kluwer: Dordrecht 1999.
- [8] M. W. Coffey, J. R. Clem, Phys. Rev. Lett. **67** (1991) 386; Phys. Rev. B **45** (1992) 9872; **45** (1992) 10527.
- [9] E. H. Brandt, Phys. Rev. Lett. **67** (1991) 2219.
- [10] A. Agliolo Gallitto, I. Ciccarello, M. Guccione, M. Li Vigni, D. Persano Adorno, Phys. Rev. B **56** (1997) 5140.
- [11] L. G. Gilchrist, P. Monceau, Philos. Mag. **18** (1968) 273.
- [12] F. Zuo, M. B. Salamon, E. D. Bukowski, J. P. Rice, D. M. Ginsberg, Phys. Rev. B **41** (1990) 6600.
- [13] A. Shibata, M. Matsumoto, K. Izawa, Y. Matsuda, S. Lee, S. Tajima, Phys. Rev. B **68** (2003) 060501(R).
- [14] A. Dulčić, D. Paar, M. Požek, V. M. Williams, S. Krämer, C. U. Jung, Min-Seok Park, Sung-Ik Lee, Phys. Rev. B **66** (2002) 014505.
- [15] A. Agliolo Gallitto, G. Bonsignore, S. Fricano, M. Guccione, M. Li Vigni, Topics in Superconductivity Research, B. P. Martins Ed., Nova Science Publishers, Inc. (New York 2005), pags. 125-143.
- [16] A. Agliolo Gallitto, M. Bonura, S. Fricano, M. Li Vigni, G. Giunchi, Physica C **404** (2003) 171.
- [17] S. Sarti, C. Amabile, E. Silva, M. Giura, R. Fastampa C. Ferdeghini, V. Ferrando, C. Tarantini, Phys. Rev. B **72** (2005) 024542.
- [18] M. Bonura, A. Agliolo Gallitto, M. Li Vigni, C. Ferdeghini, C. Tarantini, Eur. Phys. J. B **63** (2008) 165.
- [19] M. R. Eskildsen, M. Kugler, S. Tanaka, J. Jun, S. M. Kazakov, J. Karpinski, Ø. Fisher, Phys. Rev. Lett. **89** (2002) 187003.

- [20] N. Nakai, M. Ichioka, K. Machida, J. Phys. Soc. Jpn. **71** (2002) 23.
- [21] A. E. Koshelev, A. A. Golubov, Phys. Rev. Lett. **90** (2003) 177002.
- [22] A. A. Golubov, A. E. Koshelev, Phys. Rev. B **68** (2003) 104503.
- [23] A. Gurevich, Phys. Rev. B **67** (2003) 184515.
- [24] I. Pallecchi, C. Tarantini, H. U. Aebersold, V. Braccini, C. Fanciulli, C. Federghini, F. Gatti, E. Lehman, P. Manfrinetti, D. Marré, A. Palenzona, A. S. Siri, M. Vignolo, M. Putti, Phys. Rev. B **71** (2005) 212507.
- [25] C. Tarantini, H. U. Aebersold, V. Braccini, G. Celentano, C. Federghini, V. Ferrando, U. Gambardella, F. Gatti, E. Lehmann, P. Manfrinetti, D. Marré, A. Palenzona, I. Pallecchi, I. Sheikin, A. S. Siri, M. Putti, Phys. Rev. B **73** (2006) 134518.
- [26] A. Martinelli, C. Tarantini, E. Lehmann, P. Manfrinetti, A. Palenzona, I. Pallecchi, M. Putti, C. Federghini, Supercond. Sci. Technol. **21** (2008) 012001.
- [27] M. Putti, M. Affronte, C. Federghini, P. Manfrinetti, C. Tarantini, E. Lehmann, Phys. Rev. Lett. **96** (2006) 077003.
- [28] D. Daghero, A. Calzolari, G. A. Ummarino, M. Tortello, R. S. Gonnelli, V. A. Stephanov, C. Tarantini, P. Manfrinetti, E. Lehmann, Phys. Rev. B **74** (2006) 174519.
- [29] J. M. Rowell, Supercond. Sci. Technol. **16** (2003) R17.
- [30] L. Ji, M. S. Rzchowski, N. Anand, M. Tinkham, Phys. Rev. B **47** (1993) 470.
- [31] B. A. Willemsen, J. S. Derov, S. Sridhar, Phys. Rev. B **56** (1997) 11989.
- [32] M. Bonura, A. Agliolo Gallitto, M. Li Vigni, Eur. Phys. J. B **53** (2006) 315.
- [33] M. Bonura, E. Di Gennaro, A. Agliolo Gallitto, M. Li Vigni, Eur. Phys. J. B **52** (2006) 459.
- [34] J. Bardeen, M. J. Stephen, Phys. Rev. **140** (1965) A1197.
- [35] D. H. Wu, S. Sridhar, Phys. Rev. Lett. **65** (1990) 2074.
- [36] M. Eisterer, M. Zehetmayer, and H. W. Weber, Phys. Rev. Lett. **90** (2003) 247002.
- [37] G. K. Perkins, Y. Bugoslavsky, A. D. Caplin, J. Moore, T. J. Tate, R. Gwilliam, J. Jun, S. M. Kazakov, J. Karpinzki, L. F. Cohen, Supercond. Sci. Technol. **17** (2004) 232.